Hydrologic processes of groundwater in a small monsoon-influenced mountainous watershed

Ruiqiang Yuan, Shiqin Wang, Lihu Yang, Jianrong Liu, Peng Wang and Xianfang Song

ABSTRACT

Mountain block recharge is the least well quantified owing to the lack of a thorough understanding of mountain block hydrological processes. Observations of spatio-temporal variations of groundwater were employed to clarify hydrologic processes in a semi-arid mountainous watershed of northern China. Results showed that the annual feeding rate of precipitation changed between 21% and 40%. However, infiltration of precipitation was mainly drained as interflow on slopes and recharged into the mountain valley as focused recharge. As a result, the mean correlation coefficient between precipitation and groundwater level was only 0.20 and seasonal variations were reduced. Mountain slope is essentially impermeable with no bedrock percolation under arid circumstances. Only a bedrock percolation event occurred after multiple closely-spaced heavy rains during the four-year observation, which induced a local rapid ascending of the water table and an enhanced lateral recharge from upgradient watersheds. The influence of the enhanced lateral recharge lasted three years, suggesting a huge groundwater catchment overcoming local watershed divides in mountain blocks. The average of the gradual recession of the water table was 5.1 mm/d with a maximum of 11.4 mm/d in the beginning stage. Both interflow and bedrock percolation are important. Our results highlight the changeability of hydrologic processes in mountain watersheds.

Key words | bedrock percolation, groundwater recharge, hydrologic processes, mountain block recharge, mountainous watershed, North China Plain

Ruiqiang Yuan (corresponding author)
College of Environment and Resources,
Shanxi University,
Taiyuan 030006,
China
E-mail: *rqyuan@sxu.edu.cn*

Shiqin Wang
Center for Agricultural Resources Research,
Institute of Genetics and Developmental Biology, CAS,
Shijiazhuang 050021,
China

Lihu Yang
Jianrong Liu
Xianfang Song
Key Laboratory of Water Cycle and Related Land Surface Processes,
Institute of Geographic Sciences and Natural Resources Research, CAS,
Beijing 100101,
China

Peng Wang
School of Geography and Environment,
Jiangxi Normal University,
Nanchang 330022,
China

INTRODUCTION

Surface water is usually limited and inconsistent in semi-arid and arid regions. Groundwater offers a reliable source of water. Mountains often receive more precipitation than the adjacent lowlands due to orographic effects (Wilson & Guan 2004) and produce a considerable mountain front recharge (MFR) to adjacent basins (Manning & Solomon 2003; Gleeson & Manning 2008; Aishlin & McNamara 2011; Ajami *et al.* 2011). MFR is often divided into two components: (1) subsurface inflow from the adjacent mountains; and (2) infiltration from streams near the mountain front. The subsurface inflow forms 45% of recharge to the basin aquifers in humid southwestern British Columbia (Doyle *et al.* 2015). However, basin aquifers are recharged through infiltration from streams and not the subsurface inflow in the Adelaide Plains basin, South Australia (Bresciani *et al.* 2018). In addition, reservoir seepage accounts for a large proportion of mountain-front recharge (Li *et al.* 2017). Research on hydrologic processes of mountain groundwater is needed to improve the understanding of MFR.

Although mountainous terrain occupies a significant portion of the Earth's land surface, hydrologic processes in mountain watersheds are still poorly understood. Mountain-block hydrology examines all hydrologic processes in the mountain block above the mountain front (Wilson & Guan 2004). Some studies tried to build a more thorough understanding of hydrologic processes on the basis of long-

doi: 10.2166/nh.2018.030

term observations (Carling *et al.* 2012; Inamdar *et al.* 2013; Chiogna *et al.* 2014; Templeton *et al.* 2014). Models (Khazaei *et al.* 2003; Smerdon *et al.* 2009; Andreu *et al.* 2012) and environmental tracers (Manning & Solomon 2004, 2005; Manning 2011; Kao *et al.* 2012; Oda *et al.* 2013) were employed. Fault systems complicate the groundwater flow (Yuan *et al.* 2011). Topographic uniqueness influences the amounts of mountain block recharge (MBR) (Welch & Allen 2012). Large values of groundwater recharge were observed (Manning & Solomon 2004; Liu & Yamanaka 2012). The relationship of rainfall and water level data deciphers the recharge process (Panda *et al.* 2017). The depth dependence of K is critical for quantifying hydrologic partitioning between baseflow and MBR (Yao *et al.* 2017). Trenched hillslopes received more recharge compared with unaltered hillslopes (Somers *et al.* 2018). Although significant efforts were made, substantial MBR to intermountain basins is plausible. The relative importance of vertical bedrock percolation versus lateral interflow is debatable. The complexities of hydrologic processes of groundwater originating from geological conditions of mountain blocks needs to be clarified.

Long-term records of groundwater regimes provide a broad overview of hydrologic processes and a better understanding of the complexities of the hydrologic system in mountain blocks. Unfortunately, only limited data were available, which makes improving the estimation and understanding of MBR and MFR particularly challenging. This study employed long-term and comprehensive hydrologic observations in a semi-arid small mountain watershed to examine hydrologic processes and recharge in mountain blocks. The principal aim is to clarify the relative importance of vertical bedrock percolation versus lateral interflow and to discover the components of recharge to groundwater of a small mountainous watershed. The data in the paper are valuable in advancing the understanding of mountain groundwater and in achieving a better estimation of MBR and MFR.

STUDY AREA AND METHOD

Study area

The Chongling Creek Watershed is located in the transition zone of the Taihang Mountains and the North China Plain (115.3907°E, 39.3868°N). The northwest–southeast trending watershed has a length of 5.1 km and an area of 6.2 km^2 with an altitude range of 80–280 m. It is bounded by an upland plateau and mountains that rise more than 2,000 m to the west, facing the piedmont plain of the North China Plain to the east (Figure 1). The land cover is mainly woodland (42.2%) and grassland (38.4%). Farmland only occupies 1.8% of the area in the watershed, distributed along the river terrace (Data Sharing Infrastructure of Earth System Science, China).

The study area is characterized by a semi-arid, warm temperate, continental monsoon climate, with an average annual air temperature of 11.6°. The annual precipitation ranges from 257 to 889 mm with an average of 550 mm during 1966–2009 (meteorological data are from unpublished data of the local meteorological station). Over 70% of the precipitation is concentrated in the rainy season from June to August. The Chongling Creek has been dry since 2000.

Bedrock is generally exposed at elevations greater than 100 m and is comprised of limestone and marble in the north, granitic gneiss in the middle and conglomerate in the south of the watershed. The weathered layer is no

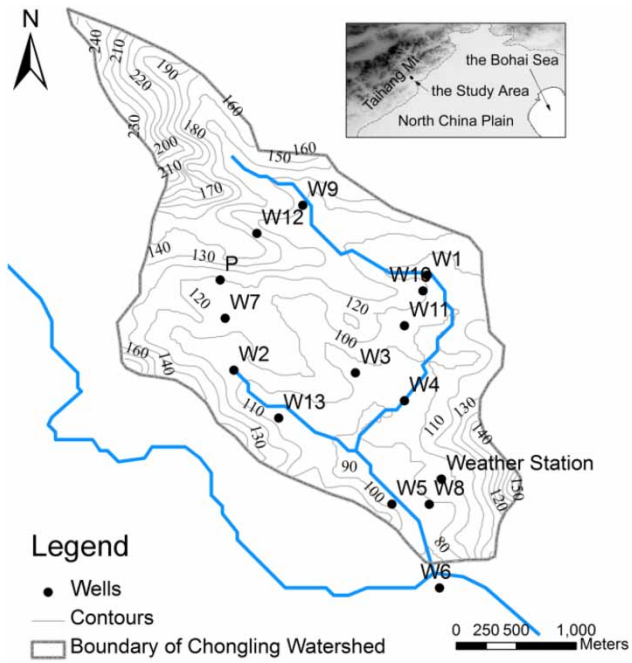

Figure 1 | Site map showing the major topographic and hydrologic features of the Chongling Creek watershed. The contour map was derived from the ASTER GDEM that is a product of METI and NASA.

more than 3 m in depth. The valley bottom is filled with unconsolidated sediments from repeated alluvial processes. Soil in the area is mainly sandy loam and loess, which has accumulated in the valleys up to depths of 1–2 m. The shallow groundwater occurs in fissured bedrock and basin-fill sediments.

Method

Eight domestic wells (W1–W8) were used to record the groundwater regime (Figure 1). All wells disclose fractured bedrock with a weathered crust on the top. The thickness of the weathered crust is about 1 m in the wells. Wells W3, W7 and W8 are situated on slopes; W1, W2 and W4 are located on the slope foot; and W5 and W6 lie on the valley bottom. Wells W1–W6 were monitored manually for depth to water table. A sensor (CTD Diver, Eijkelkamp) was set up in W7 where conductivity, temperature and water depth were measured automatically. Another sensor (Micro Diver, Eijkelkamp) was installed in W8 for recording the depth to the water table (Table 1). A meteorological station was built in the valley where meteorological data have been recorded since 2003 (Figure 1). In the watershed, V-type weirs were set on the outlet of the watershed to monitor the runoff generation every hour during the study period.

Groundwater samples were collected for cations and stable water isotopes analyses from January 2008 to October 2009 for W2, W6 and from June 2009 to October 2009 for W1, W5. Field surveys were carried out in March and September 2008 and June 2009. Groundwater was surveyed (T, pH, EC and ORP) and samples were collected from the wells for ions. Collections of precipitation samples were conducted for stable water isotopes from 2008 to 2009. Samples were filtered through a 0.45 μm membrane and filled 50 mL polyethylene bottles with double lids.

Major ions and isotopic compositions of water samples were analyzed in the laboratory of the Institute of Geographic Sciences and Natural Resources Research, Chinese Academy of Sciences. All samples were stored in the cold and dark until analysis. The chemical composition was characterized by ICP-OES for cations (Perkin Elmer Optime 5300DV) with a precision of 1 mg/L and by ion

Table 1 | Observation wells. W11 is a borehole with a 6-meter long screen section installed 37 m under the ground. Other wells are open wells

Observation and sampling sites	Altitude (m)	Location[a]	Well depth (m)	Monitoring periods	Monitoring intervals
W1	104	S	3	11/2005–10/2009	10 days for dry seasons and 5 days for rainy seasons
W2	102	S	3		
W3	101	S	8		
W4	92	S	4		
W5	88	V	6		
W6	78	V	6		
W7	113	S	9	5/2004–3/2005 12/2005–11/2006 11/2007–3/2008	30 min
W8	87	V	6	3/2005–6/2005 9/2005–12/2005 8/2006–1/2007 4/2007–1/2007 3/2008–5/2008	30 min 30 min 1 hour 1 hour 1 hour
W9	127	S	2	–	–
W10	113	S	11	–	–
W11	102	S	43	–	–
W12	137	S	–	–	–
W13	93	S	4	–	–

[a]S, slope; V, valley bottom.

chromatography (Shimadzu LC-10A) for anions with a precision of 0.1 mg/L. Hydrogen and oxygen isotopic compositions of the water samples were analyzed by the Isotope Ratio Mass Spectrometer (Finnigan MAT-253). The δD and $\delta^{18}O$ measurements were reproducible to ±1.0 and ±0.2‰ respectively.

Nonparametric Mann–Kendall test (Klaus *et al.* 2015) and Sen's slope method (Odongo *et al.* 2015) were employed to reveal trends of water table depth. Correlation analyses of time series including water table depth and precipitation were made to discover relevance in time domain. Fourier transforms were employed producing the periodograms of time series to show similarity in the frequency domain. The above mathematical analyses were achieved by programming under the Matlab environment.

RESULTS AND DISCUSSION

Distinct spatio-temporal patterns of groundwater

Groundwater was alkalescent and slightly mineralized with an average EC value of 68.3 mS/m in the watershed (Table 2). The hydrogeochemical type of groundwater was Ca-HCO_3 type. Ca^{2+} and Mg^{2+} were the dominant cations accounting for about 90% during the observation from January 2008 to October 2009, although the concentration of Ca^{2+} fluctuated greatly in groundwater (Figure 2). The δD and $\delta^{18}O$ values of groundwater samples plotted closely around the averages of precipitation (−7.48‰ for $\delta^{18}O$ and −56.3‰ for δD) and lay on the LWML (Figure 3). Although precipitation depletes heavy isotopes in winter and enriches them in summer, the seasonality was not presented in the groundwater system based on the two-year observation. It is inferred that the groundwater is meteorologically originated and well mixed to smooth seasonal isotopic variation. Therefore, there is no quick cycled groundwater with a transit time shorter than the seasonal period.

Spatio-temporal variance of groundwater table depth was distinct between slopes and the valley bottom (Figure 4). First, narrow peaks of water table depth mainly occurred in the valley bottom (W5 and W6) indicating a notable recharge. Second, standard deviations and ranges of water table depth variability and the averages were obviously larger in slopes than in the valley bottom (Table 3) revealing the changeful hydrologic processes. Finally, strong correlations of groundwater level cross sites on slopes and weak correlations at the valley bottom existed (Figure 5). The strongest correlation ($r = 0.82$) was found between W4 and W1. Similarly, good correlations were found between W2 and W1 ($r = 0.80$) and between W2 and W4 ($r = 0.79$). In the valley bottom, the correlation of groundwater level between W5 and W6 was weak. In addition, the spatio-temporal connection of major cations was only significant on slopes or in the valley. Correlation coefficient (r) ranged from 0.53 to 0.73 between sites on slopes and from 0.46 to 0.62 between sites in the valley. The distinct spatio-temporal pattern of groundwater regime suggested different hydrologic processes were occurring in the slopes and the valley bottom respectively.

Considerable infiltration of precipitation

The effective precipitation is usually smaller than the total precipitation in woodland, equal to the sum of throughfall and stem-flow. Based on long-term observation, throughfall P_1 and stem flow P_2 can be obtained (Table 4). The average precipitation input of the watershed P can be estimated as follows:

$$P = (P_1 + P_2) \times 42.2\% + P_t \times 57.8\% \quad (1)$$

where P_t is the total precipitation (mm); the area percentage of the woodland is 42.2%. No surface runoff was generated during the period according to the records from the V-type weirs stations. Therefore, the water balance of the studied watershed was established as follows:

$$P = ET + R_{ss} + F_d + \Delta S \quad (2)$$

where ET is the actual evapotranspiration, R_{ss} is interflow, F_d is bedrock percolation and ΔS is the change in soil water storage. Considering the long duration of water budget from 2006 to 2009, ΔS can be reasonably assumed as zero (Figure 6). According to the collected meteorological data by an automatic weather station in the site of Weather

Table 2 | Water chemistry and isotopic characteristics during the field surveys

Sites	pH			EC (mS/m)			ORP (mV)
Date	March 2008	September 2008	June 2009	March 2008	September 2008	June 2009	September 2008
W4	7.3	8.1	7.8	62.8	64.1	65.0	262
W6	8.2	7.6	7.6	60.7	56.7	61.1	243
W7	8.0	7.8	7.7	65.1	108.0	73.5	260
W8	7.5	7.5	7.6	84.5	91.3	84.6	282
W9	7.8	8.0	8.1	72.1	81.1	87.6	299
W10	8.0	8.3	8.2	55.6	57.0	55.7	292
W11	–	8.0	–	–	56.2	–	171
W12	8.0	7.6	7.8	37.2	39.1	38.6	291
W13	7.7	7.6	7.7	60.0	61.3	65.0	277

Sites	Ca^{2+}	Mg^{2+}	Na^{+}	K^{+}	HCO_3^-	Cl^-	SO_4^{2-}	NO_3^-	Ca^{2+}	Mg^{2+}	Na^{+}	K^{+}	HCO_3^-	Cl^-	SO_4^{2-}	NO_3^-
Date	September 2008								June 2009							
W4	72.4	26.1	12.7	1.1	256.2	19.1	74.5	38.6	64.4	26.9	13.4	0.9	292.8	16.8	57.2	32.1
W6	67.6	29.7	12.0	2.9	256.2	20.2	88.2	19.7	81.7	33.0	13.1	2.8	270.8	20.5	77.8	11.0
W7	139.8	29.0	19.7	3.2	175.7	77.8	109.0	147.8	78.2	21.3	16.6	2.2	215.9	36.8	84.7	81.5
W8	112.6	27.7	24.2	0.8	255.1	38.5	94.1	53.3	58.7	28.8	21.0	1.0	351.4	33.4	96.6	38.6
W9	97.0	38.3	12.6	3.5	300.1	32.4	86.7	68.8	88.3	44.4	13.6	3.2	333.1	27.4	97.9	65.3
W10	74.7	25.4	10.5	1.7	248.9	15.5	74.6	46.9	82.0	26.9	10.2	1.1	252.5	11.1	57.8	41.8
W11	46.9	21.7	11.7	1.4	158.1	12.4	75.6	42.2	–	–	–	–	–	–	–	–
W12	61.7	11.4	12.6	1.3	135.7	13.3	87.9	46.2	62.1	10.8	13.1	1.3	150.1	5.4	74.1	22.3
W13	78.5	29.0	10.7	1.8	241.6	17.4	78.3	38.4	87.8	31.7	11.4	1.4	267.2	20.6	79.7	51.7

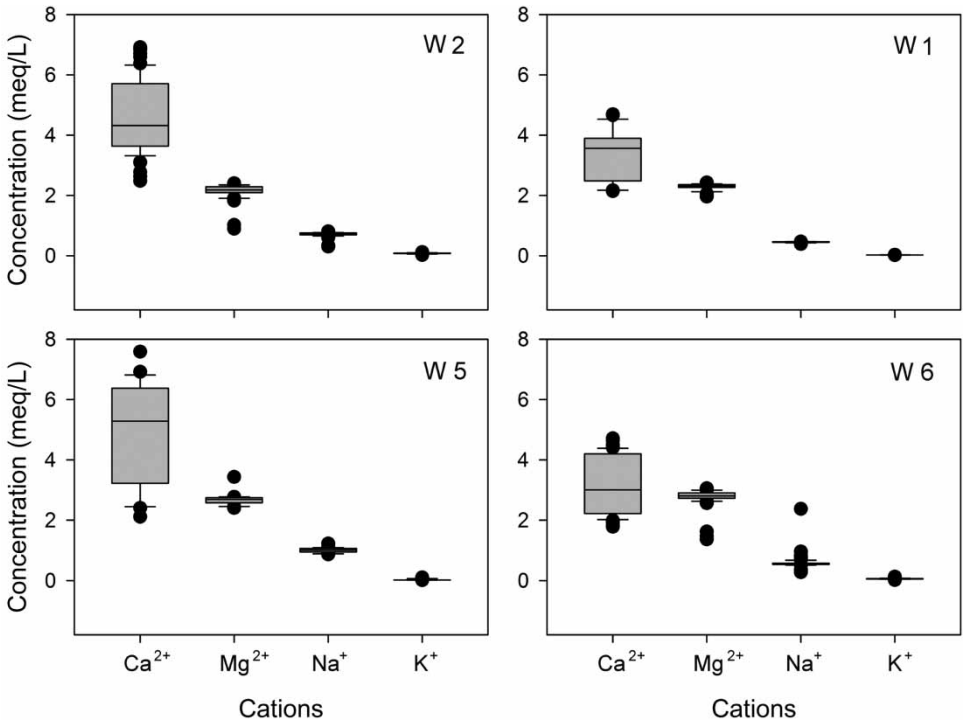

Figure 2 | Box plots of time-varying concentrations of major cations in groundwater.

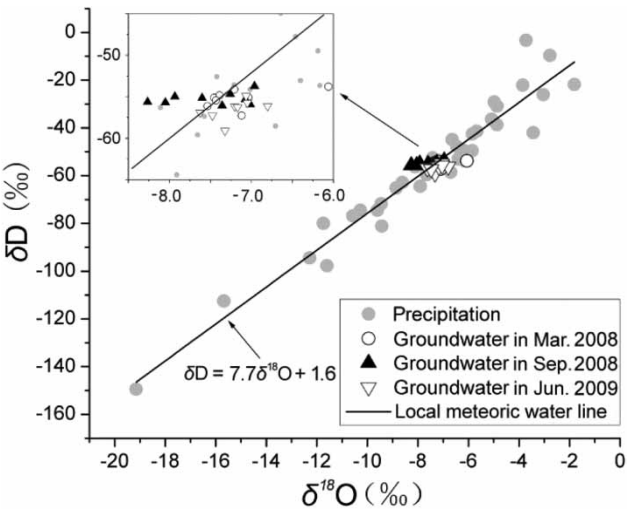

Figure 3 | Isotope composition of groundwater and precipitation.

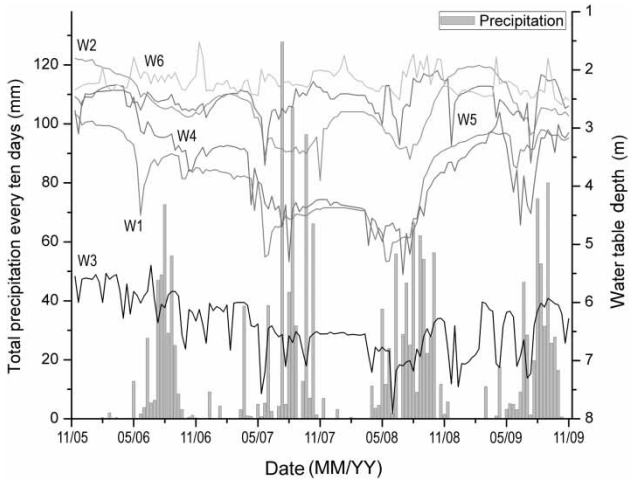

Figure 4 | Variability of water table depth and precipitation every 10 days from November 2005 to October 2009.

Station (Figure 1), the actual evapotranspiration was estimated by Hu (2012) using the FAO Penman–Monteith equation and Pei method (1989).

In mountainous terrain, a layer of higher-permeability rocks often overlies lower-permeability rocks (Gleeson & Manning 2008). Interflow usually occurs on the interface of permeability contrast. Direct recharge diffusing vertically and entering a mountain aquifer becomes a bedrock percolation, which often produces water level ascending. The sum of interflow and bedrock percolation can be calculated by the water balance residual approach (Table 5). The two parts originated from infiltration of precipitation becoming groundwater

Table 3 | Statistics for depth to water table during November 2005 to October 2009 (Unit: m)

Well	Number	Minimum	Maximum	Mean	Std. Deviation
W1	135	2.76	5.29	3.8	0.65
W2	136	1.80	3.90	2.6	0.49
W3	141	5.36	7.91	6.4	0.50
W4	137	2.25	5.52	3.6	0.75
W5	140	2.01	3.64	2.5	0.26
W6	141	1.52	2.6	2.2	0.19

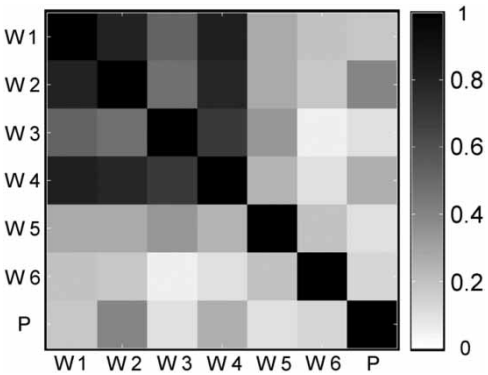

Figure 5 | Correlation matrix for time series of water table depths and precipitation. Lable P means precipitation every 10 days.

Table 4 | Throughfall and stem-flow observations in the Chongling Creek watershed (according to Hu *et al.* 2010)

Precipitation (mm)	Event number	Rainfall (mm)	Throughfall		Stem-flow	
			(mm)	(%)	(mm)	(%)
<5	18	43.7	25.3	57.7	0.1	0.2
5–10	4	22.6	16.1	71.0	0.2	0.7
10–25	6	123.8	105.6	85.3	1.2	1.0
25–50	3	96.2	84.2	87.6	1.3	1.4
>50	1	68.0	55.2	81.2	1.4	2.1

eventually. It was reported that annual infiltration coefficients of precipitation varied between 3% and 42% in semiarid mountainous basins (Scanlon *et al.* 2006). Our results show that the coefficients changed from 21% to 40% during the water budget period. The groundwater in the watershed received remarkable recharge from precipitation, which is consistent with the mountainous area recognized as the main recharge zone for regional groundwater.

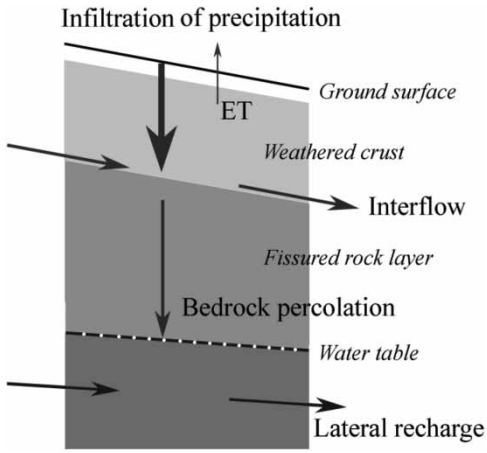

Figure 6 | Sketch of the conceptual model.

Weak correlation between precipitation and groundwater due to strong interflow

Correlation between precipitation and groundwater level was weak both in the slopes and the valley bottom. On the one hand, the mean correlation coefficient was only 0.20 (Figure 5). On the other hand, the maximum peaks for W1, W2, W3 and W4 occur at a frequency of 0.00694 Hz (Figure 7), which corresponds to 1,440 days (the entire period of observation). Therefore, the groundwater level changed without an obvious period. However, the time series of precipitation shows an obvious annual period. Despite the considerable infiltration of precipitation, the correlation between precipitation and groundwater level was weak.

Bedrock percolation reaches downwards groundwater in an aquifer producing water level ascending. However, peaks of water level were not a common phenomenon after precipitation events beneath slopes (Figures 4 and 8). The water level remains constant or even declines after rain events. It is inferred that bedrock percolation is not the main recharge mechanism for mountain blocks in this case. Precipitation infiltration was held by soil or transported downslope as interflow.

Interflow often occurs through preferential flow networks. Usually, there are two types of subsurface lateral preferential flow (LPF) network: (1) a network of connected preferential flow pathways and (2) a network of water flow along permeability contrast (Guo *et al.* 2014). Therefore, the total matrix potential gradients could be strongly lateral

Table 5 | Water budget in the Chongling Creek watershed

Year	Precipitation (mm/yr)	Effective precipitation (mm/yr)	Actual evapotranspiration[a] (mm/yr)[a]	Badrock percolation and interflow (mm/yr)
2006	358.3	313.0	236.0	77
2007	603.9	547.0	303.1	244
2008	564.0	510.0	334.2	176
2009	467.6	416.7	249.5	167

[a]Data from Hu (2012).

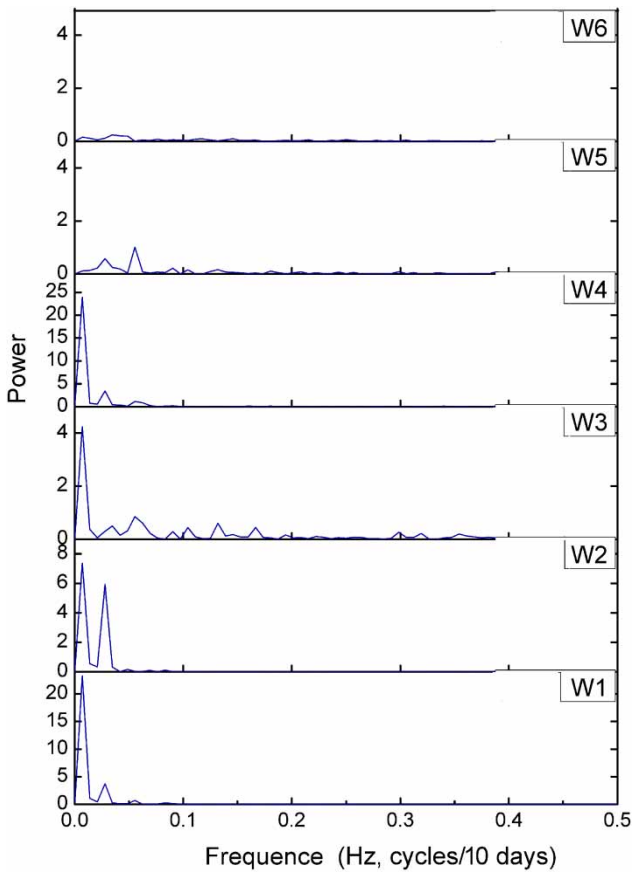

Figure 7 | Periodograms of time series of water table depth. Peaks appeared for W1, W2, W3, and W4. The maximum peaks are at a frequency of 0.00694 Hz, which is a period of about 1,440 days, namely the entire period of observation. There was no other obvious period for water table depths.

on slopes (McDonnell 1990). The lateral by-pass flow could take a dominant role in the redistribution of precipitation infiltration (Laine-Kaulio *et al.* 2014). In the study area, there are two types of preferential flow networks. A layer of weathered crust and top soil has a thickness of more than 0.7 m on slopes. The laterally orientated roots are abundant which increases the hydraulic conductivity in this layer. The weathered crust-bedrock interface offers the permeability contrast. As antecedent soil wetness increases after precipitation, preferential flow systems would begin to self-organize into complex networks. It is rational that the downslope interflow would occur along the LPF pathways. In this case, soil moisture is low due to recent drought. Most infiltration has to fill the soil water deficit first. Then infiltration can be distributed as interflows under strongly lateral matrix potential gradient. Therefore, there is usually no sufficient infiltration left to support a bedrock percolation in an arid environment. The occurrence of the bedrock percolation becomes even harder.

Based on the water level record, bedrock percolation did not occur beneath slopes most of the time. Infiltration of precipitation was drained as interflow and recharged into the valley as the seasonal focused recharge. It is considered as the main mechanism of MBR by precipitation in an arid and semi-arid watershed. Narrow valleys were the main area for groundwater receiving rainfall inputs. Therefore, the groundwater level did not respond to rainfall events beneath the slopes, but peaks of water level occurred in the valley.

Despite the focused recharge, the highest correlation coefficient between groundwater level and precipitation was only 0.41, found in the valley where pumping-induced dips were removed to calculate correlation. In the rainy season, rains mainly occurred on a scale of several hours depending on the form of the storm. The observation interval was 5 days for water table depth. The time interval of observation may be too large to achieve the exact correlation.

Rare but significant bedrock percolation

Some hillslope hydrologic studies assume that the bedrock is essentially impermeable and do not allow significant bedrock percolation. According to our observations, the

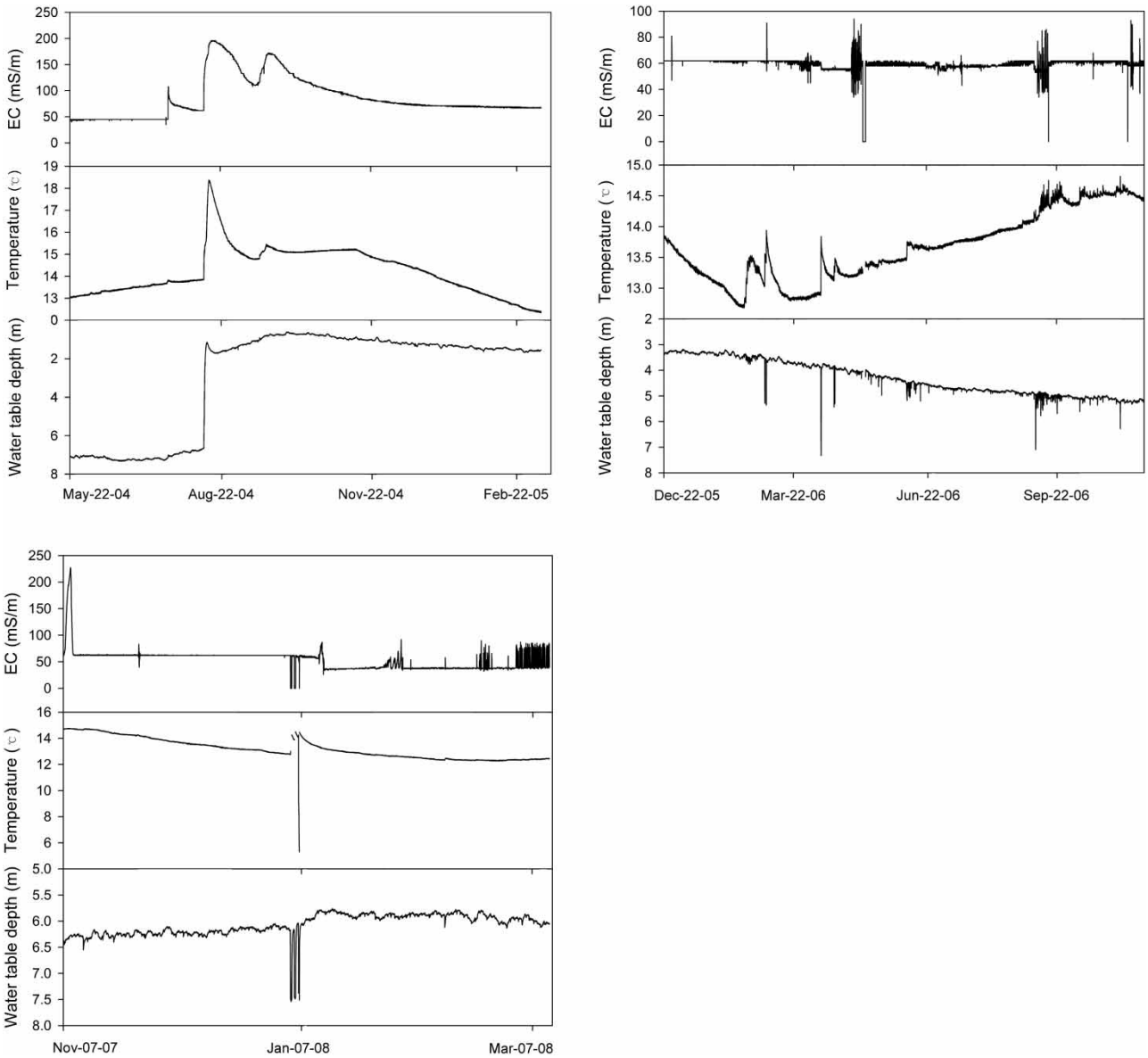

Figure 8 | Dynamic of groundwater depth, temperature and EC in well W7. Time interval is 30 minutes. A sharp rise of water level on August 12, 2004 was evidence of bed percolation. For the most part, the water level did not respond to precipitation beneath the mountain slopes even during rainy seasons (June–August). For pumping from W7, the water level declined rapidly and then stabilized at approximately 7.5 m below ground. Water level rebounded at a decreasing rate once pumping ceased.

hypothesis is applicable in an arid or semi-arid watershed. However, when rock is fractured, its permeability can increase by several orders of magnitude. Bedrock with sufficiently high bulk permeability (fracture and matrix) has the potential to allow for significant bedrock percolation (Wilson & Guan 2004). If the water is available, it can accept water at rates high enough to lead to significant bedrock percolation.

During the observation, a detailed hydrologic process of bedrock percolation was recorded at site W7 (Figure 8). Before the sharp rise (5.5 m) of water level occurred on August 12th, 2004, the water table depth was greater than 7 m. An extreme heavy rain event with a total amount of 180 mm occurred which resulted in the quick rise of water level lasting 2 days, accompanied by rapid rises of EC and temperature. The sharp rise of water level was a real-time

response to the extreme rainfall by bedrock percolation. Leaching salts from soil produced the EC peak. Higher air temperature introduced the temperature peak of groundwater. Although the water table did not ascend in the first two months of the rainy season due to long-term dry conditions, antecedent soil water deficit was compensated. Therefore a heavy rain event could produce the prominent bedrock percolation. Increased soil moisture could increase permeability of the unsaturated sediments and water head can increase to a point where the system can overcome the permeability barrier of the lower K bedrock. Bedrock percolation can still occur during temporally wet periods even in a semi-arid environment. In such cases, the occurrence of bedrock percolation requires multiple closely-spaced rainstorms.

Annual precipitation was obviously lower than 550 mm (the long-term average) from 1997 to 2003 (Figure 9). However, annual rainfall reached 642 mm in 2004 when the bedrock percolation occurred. During 2005 and 2006, annual rainfall was around 413 mm. As a result, the water table fell (Figure 4). In 2007, precipitation was sufficient and the decline of the water table ceased (Figures 4 and 8). In 2008, precipitation was still higher than average and there may be a chance to produce bedrock percolations. Unfortunately, high time-resolution data of water level missed the rainy seasons in 2007 and 2008. In addition, the data with intervals of several days were not sufficient for distinguishing responses of groundwater to rainfall events. There was no direct evidence supporting another bedrock percolation. It is rational that the vertical diffuse recharge formed by bedrock percolation was rare under semi-arid circumstances.

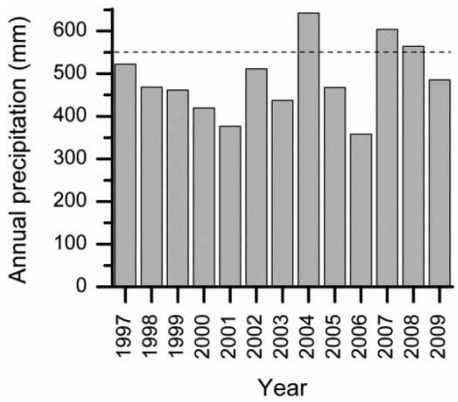

Figure 9 | Annual precipitation from 1997 to 2009. The dashed line indicates the average of annual precipitation for 1966 to 2009.

In recent studies, LPF was identified as the dominant mechanism (Laine-Kaulio *et al.* 2014), while vertical percolation was also found to play an important role even at slope angles of up to 46° (Mueller *et al.* 2014) and at the rain snow transition zone (Kormos *et al.* 2015). Lateral interflow is the dominant hydrologic process, but bedrock percolation should not be ignored in the semi-arid mountain watershed. Furthermore, the partition between the interflow and the bedrock percolation is strongly related to the correlation between groundwater level and precipitation infiltration.

Lateral recharge dominates water level fluctuation in mountain blocks

After the sharp rise of water level on August 12th, 2004, the high flow persisted from August 13th to 14th with the smallest water table depth of 1.14 m (Figure 8). After that, the water level decreased quickly. However, the arrival of the second high flow hindered the decline. The transient period lasted 2 days (August 18th–20th) with the water table depth remaining around 1.70 m, then the water level increased again. Eventually, the second high flow accompanied by a gentle wave of EC value arrived and continued from September 21st to October 26th with the smallest water table depth of 0.60 m (on October 1). The maximum value of water level of the second high flow was higher than the first high flow. The duration of the second high flow was almost 18 times longer than the first high flow. The first high flow was the result of the vertical diffuse recharge (a bedrock percolation) closely following the storm events within the watershed. The second high flow with a long duration was the result of the enhanced upgradient lateral diffuse recharge out of the small watershed.

To explore the influence of lateral recharge, increasing rates of water level were calculated based on the high-temporal resolution records. In the first stage, August 12th–14th, the ascending rate was 2.73 m/d. On the second stage, August 21st–September 21st, the rate was 3.12 cm/d. It is inferred that lateral recharge imposed a stronger and longer influence on groundwater of the watershed than that of the marked bedrock percolation. The water table

depth was more than 6.6 m before the bedrock percolation and about 6.5 m after the two-year recession (Figure 8). The influence of the enhanced lateral recharge triggered by the bedrock percolation lasted three years until the rainy season of 2007, which suggested a huge groundwater catchment in the mountainous region. This is common in a wide variety of topographic and hydrogeologic settings (Pellicer-Martínez & Martínez-Paz 2014). The recession of the lateral recharge lasted three years, dominating the groundwater hydrologic process as observed during the periods from October 26th, 2004 to March 4th, 2005 and from December 22nd, 2005 to November 20th, 2006. The decline of the water level was calculated based on the observation and the hypothesis that the recession was not interrupted. The hypothesis is reasonable according to the result of manual measurements of water level (Figure 4). The recession gradually decreased over time. The average was 5.1 mm/d with a maximum of 11.4 mm/d in the beginning stage (Table 6).

Groundwater was pumped almost daily at W8. The water level recovered very soon after the pumping ended (Figure 10). Before 2006, the average drawdown was 0.71 ± 0.23 m with a mean pumping time of 5.8 ± 3.8 hours and mean water level recovery duration lasting 7.8 ± 3.9 hours after pumping ended. After that, a more powerful pump was installed to replace the old one. The average drawdown was then 0.82 ± 0.33 m during a mean pumping time of 2.5 ± 1.4 hours and mean recovery duration of 6.5 ± 3.6 hours. Under strong pumping, the recovered water level only wavered slightly during the four-year observation. The focused recharge from slopes was usually ephemeral. Only the upgradient lateral recharge from the small watershed can support a stable and strong groundwater flow to the valley bottom.

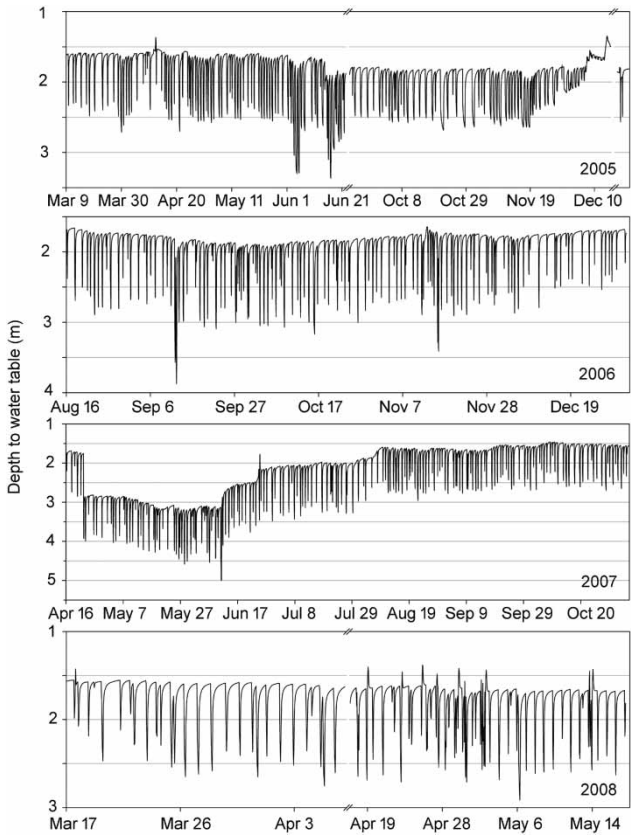

Figure 10 | Dynamic of water table depth in well W8. Observation occurred each hour. Groundwater was pumped almost daily. The water level recovered very soon after the ceasing of pumping events. Peaks formed by water level rebounds were detected after recovering. Recovered water level generally fluctuated between the depths of 1.5 to 2.0 m without any trend detected. A high water level period occurred in December 2005. During the period, the water level experienced two sudden increases due to human interference. Those data were ignored.

Table 6 | Rates of water level decline for 2004–2007 in W7

Periods	Water level decline (m)	Time (day)	Average rate of decline (mm/d)	Comments
10/26/04–03/04/05	0.828	129	6.4	Measured
03/04/05–12/22/05	1.849	293	6.3	Inferred
12/22/05–11/20/06	1.799	333	5.4	Measured
11/20/06–11/07/07	1.176	352	3.3	Inferred
10/26/04–11/26/04	0.342	30	11.4	Measured high flow recession
10/26/04–11/07/07	5.652	1,107	5.1	On the whole

During the observation period, annual precipitation decreased before 2007. As a result, the water table depths of W1, W2, W3 and W4 showed an increasing trend with gradients of 4.2–8.1 cm/month before August 2008 (Table 7), suggesting a declined lateral recharge. Consequently, the lateral recharge is the dominating groundwater source for the Chongling Creek watershed, determining the fluctuation of water level. The lateral recharge changed following the variation of annual precipitation with a time lag induced by the huge groundwater catchment.

Table 7 | Results of Mann–Kendall test and Sen's slope estimate of water table depth

	November 2005 to July 2008		August 2008 to November 2009	
Sites	Mann-Kendall test	Sen's (cm/month)	Mann-Kendall test	Sen's (cm/month)
W1	Upward trend	6.3	Downward trend	−3.9
W2	Upward trend	4.2	No significant trend	–
W3	Upward trend	4.2	No significant trend	–
W4	Upward trend	8.1	Downward trend	−6.9
W5	No significant trend	–	Upward trend detected	3.0
W6	No significant trend	–	Upward trend detected	3.0

Flow paths with various lengths can occur in mountain blocks. In intermediate and regional flow systems, groundwater discharges in a drainage basin down gradient from the basin where it recharged, which is the interbasin groundwater flow. Bedrock percolation produces a vertical diffuse recharge into mountain blocks, and interbasin groundwater flow formed lateral diffuse recharge. The lateral recharge came from the upgradient groundwater in deep bedrock aquifer, which indicated that groundwater flow could overcome local watershed divides in the Taihang Mountains block. The same evidence was found in the Daisen Mountains block (Fujimoto *et al.* 2016).

CONCLUSIONS

Hydrologic processes are closely related to dry/wet circumstances in the semi-arid mountain watershed. In this semi-arid monsoon-influenced mountainous watershed, groundwater is meteorologically originated with annual infiltration coefficients of precipitation ranging from 21% to 40%. However, correlation between precipitation and groundwater level was weak both in the slopes and the valley bottom, and seasonal variations were smoothed in groundwater. The reason is that bedrock percolation did not occur most of the time and infiltration seldom arrived at bedrock aquifer. Precipitation infiltration was drained as interflow and recharged into the valley. Therefore, the groundwater level did not respond to the rainfall event beneath slopes, but peaks of water level occurred in the valley.

Spatio-temporal variance of groundwater table depth was distinct between slopes and the valley bottom, suggesting the different hydrologic processes occurring in the slopes and the valley bottom respectively. Some hillslope hydrologic studies assume that the bedrock is essentially impermeable and do not allow significant bedrock percolation. The hypothesis is applicable most of the time in the semi-arid watershed due to the rare vertical diffuse recharge formed by bedrock percolation. Lateral recharge is the main support for the bedrock aquifer. However, bedrock percolation can still occur after multiple closely-spaced rainstorms, even in a semi-arid environment. In this watershed, both interflow and bedrock percolation are important. Valley bottom sediments gain a stable and strong recharge, mainly from interflow and upgradient lateral recharge.

A significant bedrock percolation would induce a local rapid ascending of water table and an enhanced lateral recharge from upgradient watersheds. The interbasin lateral recharge imposed a stronger and longer influence on groundwater of the watershed than that of the local bedrock percolation. The influence of the enhanced lateral recharge lasted three years, suggesting a huge groundwater catchment overcoming local watershed divides in mountain blocks. The average of the gradual recession of the water level was 5.1 mm/d with a maximum of 11.4 mm/d in the beginning stage.

ACKNOWLEDGEMENTS

This work was financially supported by the National Natural Science Foundation of China (No. 41301033) and by the project of the Institute of Geographical Sciences and Natural Resources Research (2012ZD003). The authors thank the Water and Soil Conservation Station of Baoding for research support, especially Guangying Zhang and Shengbao Wang for field survey assistance. We are grateful to Dr Shanshan Hu for sharing important data.

REFERENCES

Aishlin, P. & McNamara, J. P. 2011 Bedrock infiltration and mountain block recharge accounting using chloride mass balance. *Hydrol. Process.* **25** (12), 1934–1948.

Ajami, H., Troch, P. A., Maddock, T., Meixner, T. & Eastoe, C. 2011 Quantifying mountain block recharge by means of catchment-scale storage-discharge relationships. *Water Resour. Res.* **47** (4), 309–314.

Andreu, J. M., Alcalá, F. J., Vallejos, Á. & Pulido-Bosch, A. 2012 Recharge to mountainous carbonated aquifers in SE Spain: different approaches and new challenges. *J. Arid Environ.* **75** (12), 1262–1270.

Bresciani, E., Cranswick, R. H., Banks, E. W., Batlle-Aguilar, J., Cook, P. G. & Batelaan, O. 2018 Using hydraulic head, chloride and electrical conductivity data to distinguish between mountain-front and mountain-block recharge to basin aquifers. *Hydrol. Earth Syst. Sci.* **22** (2), 1629–1648.

Carling, G. T., Mayo, A. L., Tingey, D. & Bruthans, J. 2012 Mechanisms, timing, and rates of arid region mountain front recharge. *J. Hydrol.* **428–429**, 15–31.

Chiogna, G., Santoni, E., Camin, F., Tonon, A., Majone, B., Trenti, A. & Bellin, A. 2014 Stable isotope characterization of the Vermigliana catchment. *J. Hydrol.* **509**, 295–305.

Doyle, J. M., Gleeson, T., Manning, A. H. & Mayer, K. U. 2015 Using noble gas tracers to constrain a groundwater flow model with recharge elevations: a novel approach for mountainous terrain. *Water Resour. Res.* **51** (10), 8094–8113.

Fujimoto, M., Ohte, N., Kawasaki, M., Osaka, K. & Itoh, M. 2016 Influence of bedrock groundwater on streamflow characteristics in a volcanic catchment. *Hydrol. Process.* **30** (4), 558–572.

Gleeson, T. & Manning, A. H. 2008 Regional groundwater flow in mountainous terrain: three-dimensional simulations of topographic and hydrogeologic controls. *Water Resour. Res.* **44** (10), W10403.

Guo, L., Chen, J. & Lin, H. 2014 Subsurface lateral preferential flow network revealed by time-lapse ground-penetrating radar in a hillslope. *Water Resour. Res.* **50** (12), 9127–9147.

Hu, S. 2012 *Water Cycle Mechanism and Modeling in the Baiyangdian Lake Basin Under Changing Environment*. PhD Dissentation, Graduate School of Chinese Academy of Sciences, Beijing (in Chinese with English abstract).

Hu, S., Yu, J., Hu, K. & Jin, M. 2010 Impacts of Chinese Pine plantations on rainfall redistribution processes: a case study for the mountainous area of North China. *Acta Ecol. Sin.* **30** (7), 1751–1757 (in Chinese with English abstract).

Inamdar, S., Dhillon, G., Singh, S., Dutta, S., Levia, D., Scott, D., Mitchell, M., Van Stan, J. & McHale, P. 2013 Temporal variation in end-member chemistry and its influence on runoff mixing patterns in a forested, piedmont catchment. *Water Resour. Res.* **49**, 1828–1844.

Kao, Y. H., Liu, C. W., Wang, S. W. & Lee, C. H. 2012 Estimating mountain block recharge to downstream alluvial aquifers from standard methods. *J. Hydrol.* **426–427**, 93–102.

Khazaei, E., Spink, A. E. F. & Warner, J. W. 2003 A catchment water balance model for estimating groundwater recharge in arid and semiarid regions of south-east Iran. *Hydrogeol. J.* **11**, 333–342.

Klaus, J., Chun, K. P. & Stumpp, C. 2015 Temporal trends in δ18o composition of precipitation in Germany: insights from time series modelling and trend analysis. *Hydrol. Process.* **29** (12), 2668–2680.

Kormos, P. R., McNamaraa, J. P., Seyfriedb, M. S., Marshalla, H. P., Marksb, D. & Floresa, A. N. 2015 Bedrock infiltration estimates from a catchment water storage-based modeling approach in the rain snow transition zone. *J. Hydrol.* **525**, 231–248.

Laine-Kaulio, H., Backnäs, S., Karvonen, T., Koivusalo, H. & McDonnell, J. J. 2014 Lateral subsurface stormflow and solute transport in a forested hillslope: a combined measurement and modeling approach. *Water Resour. Res.* **50** (10), 8159–8178.

Li, X., Ye, S., Wang, L. & Jiangyi, Z. 2017 Tracing groundwater recharge sources beneath a reservoir on a mountain-front plain using hydrochemistry and stable isotopes. *Water Sci. Technol.* **17** (5), 1447–1457.

Liu, Y. & Yamanaka, T. 2012 Tracing groundwater recharge sources in a mountain-plain transitional area using stable isotopes and hydrochemistry. *J. Hydrol.* **464–465**, 116–126.

Manning, A. H. 2011 Mountain-block recharge, present and past, in the eastern Española Basin, New Mexico, USA. *Hydrogeol. J.* **19** (2), 379–397.

Manning, A. H. & Solomon, D. K. 2003 Using noble gases to investigate mountain-front recharge. *J. Hydrol.* **275** (3–4), 194–207.

Manning, A. H. & Solomon, D. K. 2004 Constraining mountain-block recharge to the Eastern Salt Lake valley, Utah with dissolved noble gas and tritium data. In: *Groundwater Recharge in A Desert Environment: The Southwestern United States* (J. F. Hogan, F. M. Phillips & B. R. Scanlon, eds). American Geophysical Union, Washington, DC, USA, pp. 139–158.

Manning, A. H. & Solomon, D. K. 2005 An integrated environmental tracer approach to characterizing groundwater circulation in a mountain block. *Water Resour. Res.* **41** (12), S12412.

McDonnell, J. J. 1990 A rationale for old water discharge through macropores in a steep, humid catchment. *Water Resour. Res.* **26** (11), 2821–2832.

Mueller, M. H., Alaoui, A., Kuells, C., Leistert, H., Meusburger, K., Stumpp, C., Weiler, M. & Alewell, C. 2014 Tracking water pathways in steep hillslopes by δ18o depth profiles of soil water. *J. Hydrol.* **519** (Part A), 340–352.

Oda, T., Suzuki, M., Egusa, T. & Uchiyama, Y. 2013 Effect of bedrock flow on catchment rainfall-runoff characteristics and the water balance in forested catchments in Tanzawa Mountains, Japan. *Hydrol. Process.* **27** (26), 3864–3872.

Odongo, V. O., Christiaan, V. D. T., Van Oel, P. R., Meins, F. M. & Becht, R. 2015 Characterisation of hydroclimatological trends

and variability in the Lake Naivasha basin, Kenya. *Hydrol. Process.* **29** (15), 3276–3293.

Panda, B., Chidambaram, S., Ganesh, N., Adithya, V. S., Pradeep, K., Vasudevan, U., Ramanathan, A. L., Ranjan, S., Prasanna, M. V. & Paramaguru, K. 2017 A study on mountain front recharge by using integrated techniques in the hard rock aquifers of southern India. *Environ. Dev. Sustain.* 10.1007/s10668-017-9987-8.

Pei, B. X. 1989 *Measurement and Estimation of Evaporation and Transipiration*. China Meteorological Press, Beijing (in Chinese).

Pellicer-Martínez, F. & Martínez-Paz, J. M. 2014 Assessment of interbasin groundwater flows between catchments using a semi-distributed water balance model. *J. Hydrol.* **519** (Part B), 1848–1858.

Scanlon, B. R., Keese, K. E., Flint, A. L., Flint, L. E., Gaye, C. B., Edmunds, W. M. & Simmers, I. 2006 Global synthesis of groundwater recharge in semiarid and arid regions. *Hydrol. Process.* **20** (15), 3335–3370.

Smerdon, B. D., Allen, D. M., Grasby, S. E. & Berg, M. A. 2009 An approach for predicting groundwater recharge in mountainous watersheds. *J. Hydrol.* **365** (3–4), 156–172.

Somers, L. D., McKenzie, J. M., Zipper, S. C., Mark, B. G., Lagos, P. & Baraer, M. 2018 Does hillslope trenching enhance groundwater recharge and baseflow in the Peruvian Andes? *Hydrol. Process.* **32** (3), 318–331.

Templeton, R. C., Vivonia, E. R., Méndez-Barrosob, L. A., Pierinia, N. A., Andersona, C. A., Rangoc, A., Laliberted, A. S. & Scotte, R. L. 2014 High-resolution characterization of a semiarid watershed: implications on evapotranspiration estimates. *J. Hydrol.* **509**, 306–319.

Welch, L. A. & Allen, D. M. 2012 Consistency of groundwater flow patterns in mountainous topography: implications for valley bottom water replenishment and for defining groundwater flow boundaries. *Water Resour. Res.* **48**, W05526.

Wilson, J. L. & Guan, H. 2004 Mountain-block hydrology and mountain-front recharge. In: *Groundwater Recharge in A Desert Environment: The Southwestern United States, Water Sci. Appl. Ser.*, Vol. 9 (J. F. Hogan, F. M. Phillips & B. R. Scanlon, eds). AGU, Washington, DC, pp. 113–137.

Yao, Y., Zheng, C., Andrews, C., Zheng, Y., Zhang, A. & Liu, J. 2017 What controls the partitioning between baseflow and mountain block recharge in the Qinghai-Tibet Plateau? *Geophys. Res. Lett.* **44** (16), 8352–8358.

Yuan, R., Song, X., Zhang, Y., Han, D., Wang, S. & Tang, C. 2011 Using major ions and stable isotopes to characterize recharge regime of a fault-influenced aquifer in Beiyishui River watershed, North China Plain. *J. Hydrol.* **405** (3–4), 512–521.

First received 15 February 2018; accepted in revised form 1 June 2018. Available online 22 June 2018